Network efficiency as a classifier for aging in resting state fMRI

Jaime Gomez-Ramirez, Yujie Li, Qiong Wu, Xiaoyu Tang, Jinglong Wu

Abstract Here we study network robustness i.e., resilience to perturbations, in resting state functional connectivity networks (R-fMRI). We investigate the effect of the lesioning of indiviudual brain regions and networks of regions in young and elder subjects. We apply analytic measures of network communication efficiency in the human brain to make reasonable guesses about compensatory mechanisms elicited in aging. A new theoretical framework to investigate network invariance under perturbation and how it is affected by internally driven processes such as aging is provided.

Key words: resting state fMRI, network degeneration hypothesis, Markov chain, relative entropy

1 Introduction

It has been suggested that fluctuations in the BOLD signal measured in humans in resting state, represent the neuronal activity baseline and shape spatially consistent patterns [1], [2]. The slow fluctuations in the BOLD signal found in resting subjects are highly coherent within either structural or functional networks in the human brain. Functional correlation based on the synchrony of low-frequency blood flow fluctuations in resting state have been identified in the sensorimotor [3], visual [4], language [5], auditory [6] and attention [7] and the frontoparietal control system [8].

The visual identification of the overall connectivity patters in resting state functional magnetic resonance imaging (R-fMRI), has been assessed first and foremost using either model-based and model-free approaches. In the former, statistical parametric maps of brain activation are built upon voxel-wise analysis location [9]. While this approach has been successful in, for instance, the identification of motor networks [10], it shows important limitations when the seed voxel cannot be easily identified [11]. For example, in brain areas with unclear boundaries i.e., cognitive networks involved in memory or self processing operations [12]. Independent Component Analysis (ICA), on the other hand, is a model-free approach that allows separating resting fluctuations from

Biomedical Engineering Laboratory, Okayama University, Japan

other signal variations, resulting on a collection of spatial maps, one for each independent component, that represent functionally relevant networks in the brain [13]. While ICA has the advantage over model-free methods that it does not need to assume a specific temporal model of correlation between regions of interest, the functional relevance of the different components is, however, computed relative to their resemblance to a number of networks, based on criteria that are not easily formalized [14].

A third approach, complementary to the other two, which is becoming of paramount importance is the network-based approach. Graph-based techniques provide new insights into the structure function relationship in the healthy brain, aging and neuropathological disorders [15], [16], [17], [18], [19], [20], [21]. The use of graph theoretic techniques to model brain networks has shifted the emphasis from the identification of local subnetworks -default mode network, primary sensory motor network etc.- to the quantitative study of the topological and informational characteristics of large-scale brain networks. Prove of the utility of this approach is that notable proponents of a modularist vision of brain connectivity to understand cognition, such as Gazzaniga [22] has now embraced a complex brain networks approach [23], [24].

Network-based approaches to R-fMRI data have demonstrated non-trivial topological properties of functional networks in the human brain. Large-scale anatomical connectivity analysis in the mammalian brain, shows that brain topology is neither random nor regular. Instead, small world architectures [25] -highly clustered nodes connected thorough relatively short paths- have been identified in brain networks. Small world networks are not solely structural, functional networks with a small world organization have been identified in the mammal brain [26]. Small world network properties have also been consistently found across different conditions, including normal development, aging, and in various pathological conditions [16], [27], [28]. While network-based studies have been successful in delineating generic network properties, such as path length or clustering, additional work is needed in order to come to grips with the internal working of the systems underlying the network. Computational simulations of disruptions in the network architecture of resting state can give clues about normal development and pathological conditions. For example, Supekar and colleagues [29] have shown that the deterioration of small world properties such as the lowering of the cluster coefficient, affect local network connectivity, which in turn may work as a network biomarker for Alzheimer's disease. Abnormalities in small-worldness may also have a significant positive correlation in, for example, schizophrenia [30] and epilepsy [31], [32].

Transport network efficiency measures have been used to study the relationsip between structural and resting state functional connectivity [33]. The effects of lesioning in white matter connections can be studied via the simulation of the removal of individual connections from the connectome. Irimia and Van Hornreport [34], using this technique have been able to delineate "a core scaffold" or white matter network connections that when disrupted, show dramatic changes in the overall organization of the human connectome. A systematic study of the effects of simulated lesioning in R-fMRI is still missing. Here we provide efficiency and robustness measures that show a more idiosyncratic response, in elder compared to young subjects, to brain region lesioning.

The rest of the paper is structured as follows. Section 2 introduces the methodology followed in the data acquisition and reconstruction, data pre-processing, and data connectivity analysis in the young and elder conditions. Then, we build a model to study quantitatively how network robustness is affected upon the removal of nodes in the functional connectivity network in both conditions. We provide an efficiency loss metric to quantify the impact of lesioning based on [35].

The empirical and clinical implications of the theoretical model are described in the results section 3.

2 Materials and Methods

2.1 Data acquisition

Forty-two healthy volunteers separated in two groups, young (ages 21-32; mean 22.7) and elder (ages 51-59; mean ?) took part in the fMRI experiment. All subjects had normal or corrected-to-normal vision. The study was approved by the ethics committee of Okayama University, and written informed consent was obtained before the study. All subjects were imaged using a 1.5 T Philips scanner vision whole-body MRI system (Okayama University Hospital, Okayama, Japan), which was equipped with a head coil. Functional MR images were acquired during rest when subjects were instructed to keep their eyes closed and not to think of anything in particular. The imaging area consisted of 32 functional gradient-echo planar imaging (EPI) axial slices (voxel size=3x3x4 mm3, TR=3000 ms, TE=50 ms, FA=90ž, 64x64 matrix) that were used to obtain T2*-weighted fMRI images in the axial plane. We obtained 176 functional volumes and excluded the first 4 scans from analysis. Before the EPI scan, a T1-weighted 3D magnetization-prepared rapid acquisition gradient echo (MP-RAGE) sequence was acquired (TR=2300 ms, TE=2.98 ms, TI=900 ms, voxel size=1x1x1 mm3).

2.2 Data preprocessing

Data were preprocessed using Statistical Parametric Mapping software SPM8 [1] and REST v1.7 [2]. To correct for differences in slice acquisition time, all images were synchronized to the middle slice. Subsequently, images were spatially realigned to the first volume due to head motion. None of the subjects had head movements exceeding 2.5 mm on any axis or rotations greater than 2.5ž. After the correction, the imaging data were normalized to the Montreal Neurological Institute (MNI) EPI template supplied with SPM8 (resampled to 2x2x2 mm3 voxels) [3]. In order to avoid artificially introducing local spatial correlation, the normalized images were not smoothed. Finally, the resulting data were temporally band-pass filtered (0.01-0.08 Hz) to reduce the effects of low-frequency drifts and high-frequency physiological noises [36].

[1] http://www.fil.ion.ucl.ac.uk/spm/

[2] http://restfmri.net/forum/index.php

[3] http://imaging.mrc-cbu.cam.ac.uk/imaging/Templates

2.3 Anatomical parcellation

Before whole brain parcellation, several sources of spurious variance including the estimated head motion parameters, the global brain signal and the average time series in the cerebrospinal fluid and white matter regions were removed from the data through linear regression. Then, the fMRI data were parcellated into 90 regions using an automated anatomical labeling template (AAL) [37]. For each subject, the mean time series of each region was obtained by simply averaging the time series of all voxels within that region.

2.4 Brain network construction

To measure the functional connectivity among regions, we calculated the Pearson correlation coefficients between any possible pair of regional time series, and then obtained a temporal correlation matrix $(90x90)$ for each subject. We applied Fisher's r-to-z transformation to improve the normality of the correlation matrix. Then, two-tailed one-sample t-tests were performed for all the possible $4005 = \frac{90x89}{2}$ pairwise correlations across subjects to examine whether each inter-regional correlation significantly differed from zero. A Bonferroni-corrected significance level of $p < 0.001$ was further used to threshold the correlation matrix into an adjacency matrix whose element was 1 if there was significant correlation between the two brain regions and 0 otherwise. Finally, an undirected binary graph was acquired in which nodes represent brain regions and edges represent links between regions.

2.5 Information Efficiency

A quantitative understanding of network robustness, that is, functional network invariance under perturbation can shed light on the properties that mediate in developmental, aging and pathological processes in the human brain. In essence, robustness measures the capacity of the network to perform the same function before and after a perturbation. Perturbations are events, internal or external, that elicit a change in the network configuration. Possible perturbations are the obliteration of a node and a change in the connectivity between nodes. Here we perform perturbations that consist on the obliteration of one or more nodes together with and all the edges that connect the lesioned node.

The efficiency of a network is a network centrality measure that quantifies the network's reliability in transmitting information once a node or a set of nodes have being removed. One possible measure of network efficiency is the Latora and Marchiori [35] measure of network efficiency defines the efficiency in transmitting information between any two nodes (i,j) in a graph G as the inverse of the shortest path that connects them

$$\varepsilon_{ij} = \frac{1}{d_{ij}} \tag{1}$$

where d_{ij} is the shortest path length or the geodesic distance between nodes i and j. Note that when there is no path that connects the nodes i and j, $d_{ij} = \infty$, and the efficiency in the communication of the two nodes is zero, $\varepsilon_{ij} = 0$.

The efficiency of the graph G, $\Sigma(G)$, is calculated as the average of the efficiency between any two nodes ε_{ij}

$$\Sigma(G) = \frac{\sum_{i \neq j \in G} \varepsilon_{ij}}{N(N-1)} = \frac{1}{N(N-1)} \frac{1}{\sum_{i \neq j \in G} d_{ij}} \tag{2}$$

where N is the number of nodes.

We can calculate the information centrality C of any node i in a network G as the variation in the network efficiency caused by the removal of the edges incident in i. Thus, the centrality of a node i, C_i, is calculated as the difference between the efficiency of the original graph G with N nodes and E edges, $G(N,E)$, and the efficiency of the resulting graph $G(N,E-k_i)$ with N nodes and $E-k_i$ edges, where k_i denotes the set of edges incident to node i. The centrality of a node is a normalized measure of the loss in network efficiency, caused by the isolation of a node in G.

$$C_i = \frac{\Sigma(G(N,E)) - \Sigma(G(N-i,E-k_i))}{\Sigma(G(N,E))} \tag{3}$$

From equation 3, a network G is considered to be robust to a perturbation δ if the network efficiency, $\Sigma(G)$, stays close to the original value after a perturbation. Ideally $\Sigma(G(N,E)) = \Sigma(G(N,E-k_i))$ with efficiency loss or centrality of node i equals to 0. By the same token, the information centrality of a set of nodes S or the efficiency loss upon the removal of S, can be calculated as the normalized measure of the loss in network efficiency caused by the isolation of a set of nodes S in G

$$C_S = \frac{\Sigma(G(N,E)) - \Sigma(G(N-S,E-k_S))}{\Sigma(G(N,E))} \tag{4}$$

3 Results

In what follows we calculate, for both conditions, the network efficiency prior to any insult (Section 3.1), the efficiency loss after single node lesioning (Section 3.2) and the efficiency loss after lesioning specific networks of interest (Section 3.3)

3.1 Efficiency prior perturbation

The global network efficiency for unperturbed networks as defined in Equation 2 is 0.3678 for young subjects and 0.1144 for elder subjects. Thus, young subjects connectivity network is a bit more than three times (3.21) more efficient in terms of the shortest path distance between any two nodes. The the number of edges in the young condition is 718 and in the young condition is 308, the average degree connectivity are 8.97 and 4.42 respectively 1.

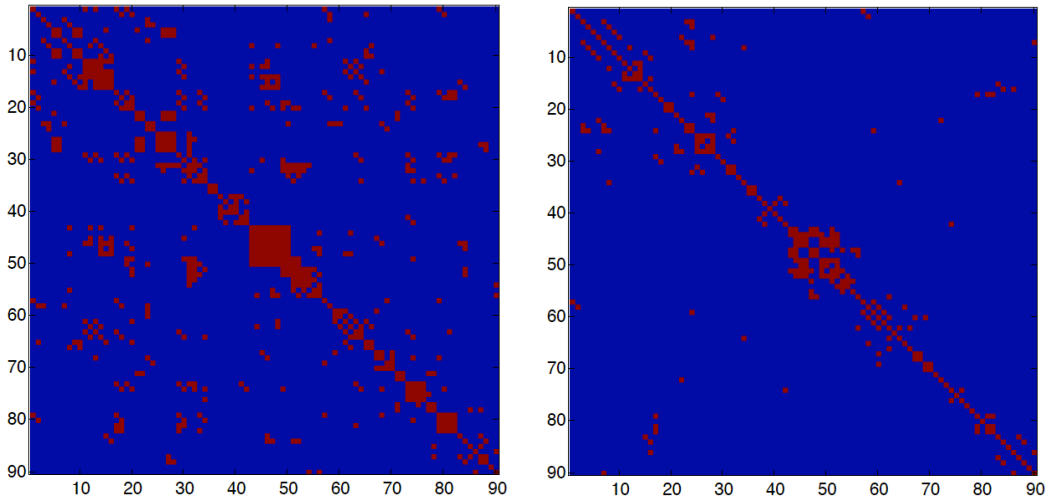

Fig. 1: (a) Adjacency matrix in the young condition. (b) Adjacency matrix old condition. The red dots prepresent connections between two nodes. In the old condition the adjacency matrix is more sparse, it has 308 edges (718 edges in the young condition)

3.2 Efficiency after single node lesioning

In order to obtain the efficiency measures described in Equations 3 and 4 we perturb the resting state network in two ways. First, using random node deletion and second targeting specific networks. In the random node deletion case, we build a population of networks perturbed by the systematic lesioning of single nodes. This is described next in Section **??**. In section **??** we target specific networks, that is, a number of networks of interest are lesioned and the efficiency loss calculated.

The population of perturbations P that result from the systematic deletion of all nodes in all possible combinations, from an initial network of N nodes, has as many networks as

$$|P| = \sum_{i=1}^{N} C(N,i) = \frac{N!}{(i!)(N-i)!}$$

For example, the population of networks that result from the deletion of one single node has 90 networks

$$\sum_{i=1}^{1} C(90,i)_{i=1} = \frac{90!}{(1!)(90-1)!} = 90$$

Similarly, the number of perturbed networks obtained by deleting two nodes in all possible ways contains 4005 networks

$$\sum_{i=1}^{2} C(90,i)_{i=2} = \frac{90!}{(2!)(90-2)!} = 4005$$

We build a distribution of the efficiency measures described in section 2 for both young and elder condition for the systematic removal of one node. Thus, in the young condition, we denote $P_{y,90}$ the distribution of networks with only one node removed, that is, $P_{y,90}$ has 90 different networks where for each one a node and its connections have been deleted. The mean of the efficiency measure for $P_{y,90}$ is 0.358. The removal of node "Inferior temporal gyrus" (89) has no effect in the efficiency, that is, the network efficiency before and after the removal has identical value. Nodes 35 and 36 ("Posterior cingulate gyrus") have also an extremely mild effect after their removal. The most significant loss in efficiency occurs with the removal of node 74 ("Lenticular nucleus, putamen") followed by node 31 ("Insula right") (Figure 2).

The average efficiency loss in the young condition is 2.44"%" with a maximum of 4.67"%" for node 74 ("Lenticular nucleus, putamen") and no efficiency loss for node 89 ("mporal pole: middle temporal gyrus"). The rationale for the different impact in the efficiency caused by the obliteration of certain nodes can be found in the connectivity degree. In general, the nodes that after their removal trigger a low efficiency loss have also low connectivity degree and those that produce a more pronounced reduction of the network efficiency tend to be more connected (Figure 3).

Similarly, for the elder condition, we denote $P_{o,90}$ the distribution of networks with only one node removed in the elder condition. The mean of the efficiency measure (equation 2) for the 90 networks obtained upon single node deletion is 0.109. As it happened in the young condition, the removal of node "Inferior temporal gyrus" (89) has no effect in the efficiency, that is, the network efficiency before and after the removal of the "Inferior temporal gyrus" has identical value. Interestingly, the removal of nodes with the lowest connectivity degree (2) have also no quantifiable effect in the network efficiency (Figure 2).

The most significant loss in efficiency occurs with the removal of node node 62 "Parietal Inf R". After the removal of this node, the efficiency loss relative to the original network is the 32.87"%". This is an interesting result since node 62 is not a highly connected node, its connectivity degree is 6. Nodes 24, 44 and 51 have more connections, connectivity degree 10, and upon their deletion the efficiency loss is not as severe as in the case of node 62. The mean efficiency loss in the elder condition after the removal of a single node is 4.61"%". The effect in the loss of efficiency triggered by the disconnection of brain areas is more stereotypical in the elder condition than in young condition, that is, the connectivity degree is a much worse predictor of efficiency loss for old than for young (Figure 3).

3.3 Efficiency after target networks lesioning

So far, we have quantified the efficiency loss due to the removal of single nodes, in what follows we investigate how efficiency is affected by removal of entire networks of interest. In particular we study the efficiency loss or centrality of nine different networks or brain structures, the Defaul

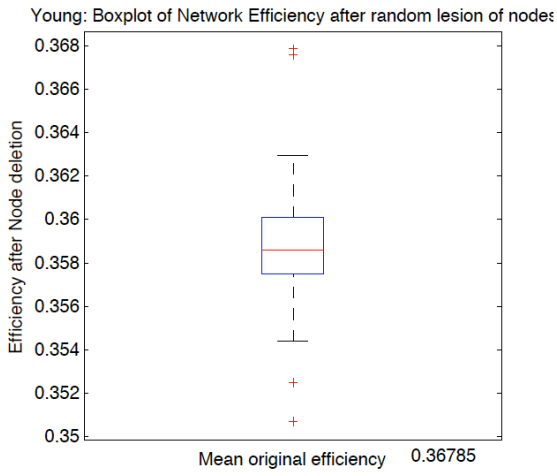

(a) Young: Efficiency after one node deletion

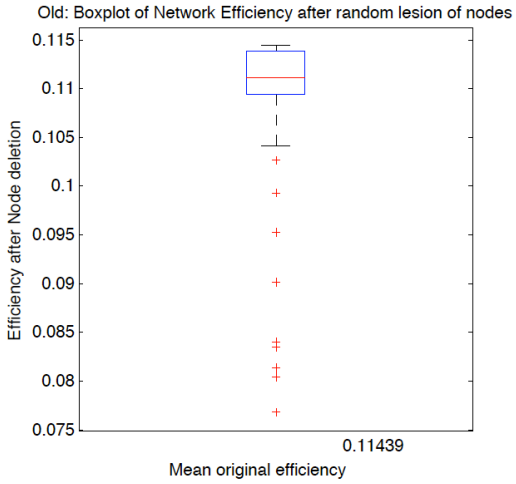

(b) Old: Efficiency after one node deletion

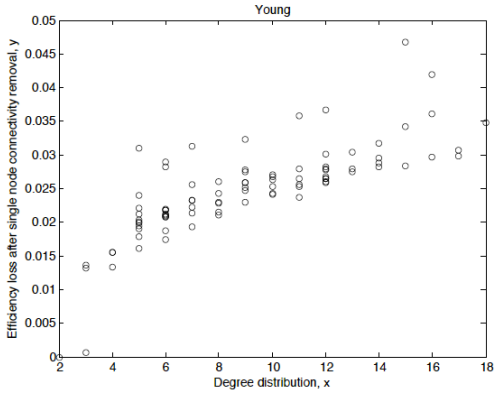

(c) Young: Degree distribution (X) Efficiency loss (Y)

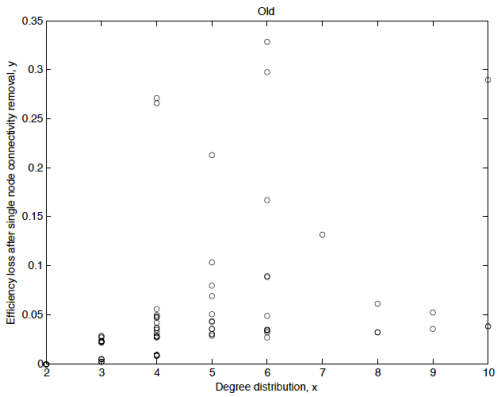

(d) Old: Degree distribution (X) Efficiency loss (Y)

Fig. 2: (a) Boxplot of network efficiency after random lesion of individual nodes. Only a very few nodes fall outside the box of the figure whose edges are the 25th and 75th percentiles. (b) Boxplot of network efficiency after random lesion of individual nodes. More nodes fall outside below the 25th percentile than in the young condition. The distribution in the elder condition is more skewed than in the young condition.(c) Degree distribution (x-axis) and efficiency loss (y-axis) after single node connectivity removal in the young condition. (d) Degree distribution (x-axis) and efficiency loss (y-axis) after single node connectivity removal in the elder condition. The linear regression in the young condition is 0.755 and in the old condition is 0.4002. The effect in the loss of efficiency triggered by the disconnection of brain areas is more stereotypical in the elder condition than in young condition.

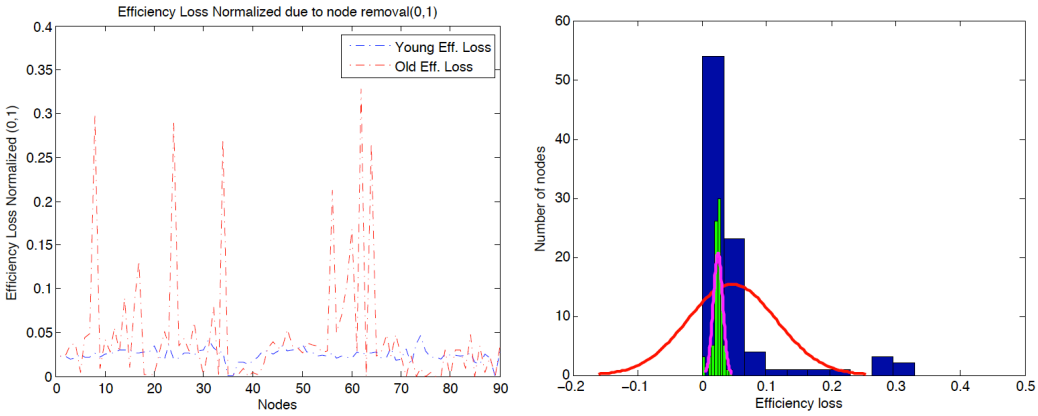

(a) Efficiency loss in young (blue) and old (red) for single node removal

(b) Frequency bars for efficiency loss in young (green) and old (blue) for single node removal

Fig. 3: (a) Efficiency loss normalized (0,1) due to the removal of each node in both elder and young condition. While in the young condition there are no nodes that upon its removal the efficiency of the resulting network drastically deteriorates, in the elder condition there are 6 nodes that upon their removal trigger a 20% or more reduction in the network efficiency. Nodes 8,29.7% 24,28.9% 34,27.1% 56,21.2% 62,32.8% 64,26.5%. (b) Distribution of efficiency loss after node removal in both young (green histogram) and elder condition (blue histogram). The efficiency loss in the young condition is narrow. The elder condition, on the other hand, has a more spread distribution of efficiency values. The range in efficiency loss in the young condition varies a 4.67% and in the elder condition varies a 32.87%

Mode Network (DMN), Visual Network, temporal lobe, frontal lobe, insula and cingulate gyrus, occipital lobe, parietal lobe, central structures and limbic structures.

The DMN is commonly considered to consist of medial prefrontal cortex (AAL 23, 24, 25, 26), posterior cingulate cortex/precuneus (AAL 35, 36/67 68) and bilateral inferior parietal lobule (AAL 61, 62). The removal of the DMN in young adults triggers an efficiency loss of the 19.6%. In the elder condition, the same procedure yields an efficiency reduction of 61.66%. It ought to be remarked that the lesioning of the 10 AAL regions that compose the DMN network, which represents the 11% of the total regions 90 regions, bring down the efficiency of the network to 61.66%. The strong efficiency reduction associated with the lesioning of the DMN is coherent with the hypothesis that there is a decrease in activity in the DMN in aging. This age-based reduction in DMN activity can trigger mechanisms that compensate the loss in DMN activity with an increase in connectivity between the DMN and other networks [38]. According to this hypothesis, the DMN becomes a more central network and upon the lesioning of the DMN a larger efficiency loss is produced. We apply the efficiency measure for lesioning of edges and we we found no significant effect of age on DMN inter-connectivity (0.16% of efficiency loss in young subjects and 0.9% in old subjects upon the disconnection of areas in different hemispheres). This result is in agreement with previous studies of aging on default mode network activity in resting state fMRI: [39]

The vision-related brain regions (hereafter called Visual) in the AAL template include left and right calcarine fissure and surrounding cortex (Nodes 45,46), left and right lingual gyrus (Nodes

47,49), left and right superior occipital gyrus (Noes 49,50), left and right middle occipital gyrus (Nodes 51, 52), left and right inferior occipital gyrus (Nodes 53, 54), left and right fusiform gyrus (Nodes 55, 56), left and right superior parietal gyrus (Nodes 59,60), and right inferior temporal gyrus (Nodes 89, 90). The removal of the Visual network in young adults triggers an efficiency loss of the 38.93% while in the elder condition the same procedure yields a 55.98%.

3.4 Efficiency after target networks lesioning of edges

4 Discussion

We have analyzed the functional connectivity in resting state of both young and elder individuals, using a perturbational approach consisting on either the systematic removal of single nodes and the removal of entire networks of interest such as the DMN and others. We have computed the loss in network efficiency upon the lesioning of brain areas. Our results expand previous works on the study of robustness of structural brain networks. Interestingly, we find that the distribution of network efficiency in the young and the elder condition show very different signatures. The functional resting state network in young adults is more robust to node removal than in elder subjects. The efficiency loss in young subjects, upon the removal of single nodes, is always below the 5% while in the elder condition the removal of individual nodes may yield a dramatic reduction of the network efficiency. The young adults are, thus, more robust to random deletion of single nodes nodes. However, when the lesioning is focused in specific brain networks rather than single regions, the efficiency loss for young subjects is in occassion higher than when the same damage is done in old subjects. For example, the disconnection of the occipital lobe, limbic structures and central structures yield a larger efficiency loss in the young condition.

In [40] applied a Support Vector Machine (SVM) linear classifier to rs-fMRI data in order to compare age-related differences in four of the major functional brain networks: the default, cingulo-opercular, fronto-parietal, and sensorimotor. With this method they detected ?connectivity hubs,? or nodes with the most significant features that influenced age classification. The best redictors of age based on SVM are not coincident with the best predictors in age using the efficiency loss method.

We test the asymmetry hypothesis by which brain activity shows a more balance activity among the two hemispheres with age, that is, the hypothesis predicts that in young individuals brain activity is more asymetric than in old indivduals. To test it we lesion sequentally the left and the right hemisphere and we calculate the efficiency loss for each case. In young individuals the difference in efficiency loss for disconnecting the hemispheres is expected to be larger than in the old condition. Aging thus, tries to compensate the reduction of activity level, for example in the DMN, by balancing the activity accross the brain. We see, on the contrary, that if one of the two hemisphere is entirely lesioned, the efficiency loss in young adults is 0.7532 when the left side is lesioned and 0.7701 when the right side is gone. The difference is 0.0169. In old sbjects, the lesioining of the right side has a more pronounced impact in the efficiency loss, 0.9121 for the removal of the right side and 0.7089 for the removal of the left side. The differece is 0.2032.

Disconnecting the DMN, left from right side, we have in young subjects with the left side gone 0.1029 efficiency loss and 0.1004 for the DMN right side gone. Difference 0.0025. For old subjects DMN left gone 0.5616 and right gone 0.0994. The difference is 0.4622. Thus, the dramatic loss in efficiency is mainly due to left side nodes.

To test the hypothesis that that the relationship between the hippocampus and the DMN tends to break down with age we lesion edges itself rather than nodes as we have done inthe previous cases. Salami et al. show that [41] elevated HC at rest may degree the degree to whoch HC interacts with other regions during memory tasks, and thus results in memory deficits. However this view is not uncontested and in it is suggested that connectivity between left and right hippocampus is negatively related to age. In our study the efficiency loss produced by the disconnection of the left and the right side of hippocampal and parahippocampal areas does not yield a reduction of efficiency loss since these areas are not connected in the old subjects (Table 1)

The degradation of fronto-striatal network in task studies has been suggested to be a driving force of memory decline in aging. The connectivity of fronto-striatal pathways are also related to self-esteem [42]. We investigate the impact of the fronto-striatal disconnection using the efficiency metric and we find that in the young condition the removal of edges that connect the frontalstratium pathways gives a reduction of efficiency of 0.37%. In the old conditions, the are no no edges connecting fornto-stratial areas and therefore there is no efficiency loss associated to this lesioning.

Table 1: Efficiency loss caused by the deletion of edges that connect brain regions in young and elder conditions. For example DMN-DMN is the deletion of the edges that connect the right and the side side of the DMN, DMN-HC the edges that connect DMN and HC, including parahippocampal areas

Network-Network Edges disconnection	Eff.loss Young	Eff.loss Old
DMN-DMN	0.64%	0.99%
HC-HC	1.43%	0.45%
HC-DMN	0.16%	0%
Frontal-Stratium	0.37%	0%

The literature reviewed here suggests that graph-based network analyses are capable of uncovering system-level changes associated with different processes in the resting brain, which could provide novel insights into the understanding of the underlying physiological mechanisms of brain function. We also highlight several potential research topics in the future. Graph theory-based approaches model the brain as a complex network in which nodes represent brain regions of interest and the edges connecting nodes represent relationship between nodes e.g., functional connectivity.

For the future we expect to establish a link between pathological lesions and the topological centrality and the efficiency of nodes studied here, and replicate our results with different imaging techniques. We intend to investigate whether, as postulated in [43] hubs of human brain networks are more likely to be anatomically abnormal than non-hubs in many brain disorders. The relevance for the network efficiency measure defined here and of the continuum decrease in DMN functional connectivity found from normal aging to mild cognitive impairment and to Alzheimer's disease (AD) may also shed light on the characterization of DMN connectivity in mental dis-

Table 2: The table shows the efficieny loss after the disconnection of different brain structures in both conditions. Interestingly, the reduction in efficiency is not always more pronounced in the elder condition. For example, the disconnection of the central stuctures (caudate nucleus, putamen, pallidum and thalamus) triggers a larger efficiency disruption in young than in old individuals. A similar situation, larger efficiency loss in young than in old, also occurs with the disconnection of the limbic structures (hippocampus, parahippocampus and amygdala) and the occipital lobe areas. The table shows the efficiency loss in both young and old condition when target networks are lesioned. The lesion consists on the obliteration of the nodes defined in the second column. The efficiency loss is larger in old adults with the execption of the occipital lobe, the central structures and the limbic structures. The reduction of efficiency in the central structures is particularly interested since in the old condition it yields only a 3.16% reduction in efficiency while in the young condition the efficiency loss for the same lesioning yoelds a reduction of 23.01%. The minor impact of the lesioning of central and limbic structures is conforming with the degradation of of fronto-stratial nework in aging [41] and the break-down between the hipicampal regions and the DMN [42]

Target Brain Structure	AAL regions	Eff.loss Young	Eff.loss Old
DMN	3 24 25 26 35 36 37 68 61 62	19.66%	61.66%
Visual areas	43 44 45 46 47 48 49 50 51 52 53 54 55 56 59 60 89 90	38.93%	55.98%
Frontal Lobe	1 2 3 4 5 6 7 8 9 10 11 12 13 14 15 16 17 18 51 52	42.83%	67.07%
Temporal Lobe	37 38 39 40 41 42 55 56 79 80 81 82 83 84 85 86 87 88 89 90	33.56%	41%
Occipital Lobe	43 44 45 46 47 48 49 50 51 52 53 54	31.71%	30.79%
Parietal Lobe	57 58 59 60 61 62 63 64 65 66 67 68	26.65%	45.64%
Insula and cingulate gyrus	3 24 25 26 35 36 37 68 61 62	18.72%	36.91%
Central structures (Caudate nucleus, putamen, pallidum, thalamus)	71 72 73 74 75 76 77 78	23.01%	3.16%
Limbic structures (hippocampus, parahippocampus, amygdala)	37 38 39 40 41 42	9.30%	1.40%

orders. For example, the lowering of DMN activity is associated with better performance on attention-demanding tasks, and DMN hyperactivity is being related to negative rumination and depression [**?**]. In addition to interplay between brain activity is relevant brain networks and efficiency measures a future libe of research is the understanding of brain metabolism with measures of informational efficiency

References

1. M. E. Raichle and D. A. Gusnard, "Intrinsic brain activity sets the stage for expression of motivated behavior," *The Journal of Comparative Neurology*, vol. 493, no. 1, pp. 167–176, 2005.
2. P. Fransson, "How default is the default mode of brain function?: Further evidence from intrinsic BOLD signal fluctuations," *Neuropsychologia*, vol. 44, no. 14, pp. 2836–2845, 2006.
3. S.-M. Kokkonen, J. Nikkinen, J. Remes, J. Kantola, T. Starck, M. Haapea, J. Tuominen, O. Tervonen, and V. Kiviniemi, "Preoperative localization of the sensorimotor area using independent component analysis of resting-state fMRI," *Magnetic resonance imaging*, vol. 27, pp. 733–740, July 2009. PMID: 19110394.
4. J. S. Damoiseaux, S. A. R. B. Rombouts, F. Barkhof, P. Scheltens, C. J. Stam, S. M. Smith, and C. F. Beckmann, "Consistent resting-state networks across healthy subjects," *Proceedings of the National Academy of Sciences of the United States of America*, vol. 103, pp. 13848–13853, Sept. 2006. PMID: 16945915.
5. M. Hampson, B. S. Peterson, P. Skudlarski, J. C. Gatenby, and J. C. Gore, "Detection of functional connectivity using temporal correlations in MR images," *Human brain mapping*, vol. 15, pp. 247–262, Apr. 2002. PMID: 11835612.
6. M. D. Hunter, S. B. Eickhoff, T. W. R. Miller, T. F. D. Farrow, I. D. Wilkinson, and P. W. R. Woodruff, "Neural activity in speech-sensitive auditory cortex during silence," *Proceedings of the National Academy of Sciences of the United States of America*, vol. 103, pp. 189–194, Jan. 2006. PMID: 16371474.
7. M. D. Fox, M. Corbetta, A. Z. Snyder, J. L. Vincent, and M. E. Raichle, "Spontaneous neuronal activity distinguishes human dorsal and ventral attention systems," *Proceedings of the National Academy of Sciences of the United States of America*, vol. 103, pp. 10046–10051, June 2006. PMID: 16788060.
8. J. L. Vincent, I. Kahn, A. Z. Snyder, M. E. Raichle, and R. L. Buckner, "Evidence for a frontoparietal control system revealed by intrinsic functional connectivity," *Journal of neurophysiology*, vol. 100, pp. 3328–3342, Dec. 2008. PMID: 18799601.
9. B. Biswal, F. Z. Yetkin, V. M. Haughton, and J. S. Hyde, "Functional connectivity in the motor cortex of resting human brain using echo-planar MRI," *Magnetic resonance in medicine: official journal of the Society of Magnetic Resonance in Medicine / Society of Magnetic Resonance in Medicine*, vol. 34, pp. 537–541, Oct. 1995. PMID: 8524021.
10. S. Robinson, G. Basso, N. Soldati, U. Sailer, J. Jovicich, L. Bruzzone, I. Kryspin-Exner, H. Bauer, and E. Moser, "A resting state network in the motor control circuit of the basal ganglia," *BMC Neuroscience*, vol. 10, p. 137, Nov. 2009.
11. J. A. Maldjian, "Functional Connectivity MR Imaging: Fact or Artifact?," *American Journal of Neuroradiology*, vol. 22, pp. 239–240, Feb. 2001.
12. A. A. Fingelkurts and A. A. Fingelkurts, "Persistent operational synchrony within brain default-mode network and self-processing operations in healthy subjects," *Brain and Cognition*, vol. 75, pp. 79–90, Mar. 2011.
13. V. D. Calhoun, J. Liu, and T. Adali, "A review of group ICA for fMRI data and ICA for joint inference of imaging, genetic, and ERP data," *NeuroImage*, vol. 45, pp. S163–172, Mar. 2009.
14. B. B. Biswal, M. Mennes, X.-N. Zuo, S. Gohel, C. Kelly, S. M. Smith, C. F. Beckmann, J. S. Adelstein, R. L. Buckner, S. Colcombe, A.-M. Dogonowski, M. Ernst, D. Fair, M. Hampson, M. J. Hoptman, J. S. Hyde, V. J. Kiviniemi, R. KÃűtter, S.-J. Li, C.-P. Lin, M. J. Lowe, C. Mackay, D. J. Madden, K. H. Madsen, D. S. Margulies, H. S. Mayberg, K. McMahon, C. S. Monk, S. H. Mostofsky, B. J. Nagel, J. J. Pekar, S. J. Peltier, S. E. Petersen, V. Riedl, S. A. R. B. Rombouts, B. Rypma, B. L. Schlaggar, S. Schmidt, R. D. Seidler, G. J. Siegle, C. Sorg, G.-J. Teng, J. Veijola, A. Villringer, M. Walter, L. Wang, X.-C. Weng, S. Whitfield-Gabrieli, P. Williamson, C. Windischberger, Y.-F. Zang, H.-Y. Zhang, F. X. Castellanos, and M. P. Milham, "Toward discovery science of human brain function," *Proceedings of the National Academy of Sciences of the United States of America*, vol. 107, pp. 4734–4739, Mar. 2010.
15. D. A. Fair, A. L. Cohen, J. D. Power, N. U. F. Dosenbach, J. A. Church, F. M. Miezin, B. L. Schlaggar, and S. E. Petersen, "Functional brain networks develop from a "local to distributed" organization," *PLoS computational biology*, vol. 5, p. e1000381, May 2009.
16. J. Wang, X. Zuo, and Y. He, "Graph-based network analysis of resting-state functional MRI," *Frontiers in Systems Neuroscience*, vol. 4, p. 16, 2010.
17. Y. He and A. Evans, "Graph theoretical modeling of brain connectivity," *Current opinion in neurology*, vol. 23, pp. 341–350, Aug. 2010. PMID: 20581686.

18. J.-H. Wang, X.-N. Zuo, S. Gohel, M. P. Milham, B. B. Biswal, and Y. He, "Graph Theoretical Analysis of Functional Brain Networks: Test-Retest Evaluation on Short- and Long-Term Resting-State Functional MRI Data," *PLoS ONE*, vol. 6, p. e21976, July 2011.
19. Q. Yu, J. Sui, S. Rachakonda, H. He, W. Gruner, G. Pearlson, K. A. Kiehl, and V. D. Calhoun, "Altered Topological Properties of Functional Network Connectivity in Schizophrenia during Resting State: A Small-World Brain Network Study," *PLoS ONE*, vol. 6, p. e25423, Sept. 2011.
20. M. R. Brier, J. B. Thomas, A. M. Fagan, J. Hassenstab, D. M. Holtzman, T. L. Benzinger, J. C. Morris, and B. M. Ances, "Functional connectivity and graph theory in preclinical Alzheimer's disease," *Neurobiology of Aging*, vol. 35, pp. 757–768, Apr. 2014.
21. R. Sala-Llonch, C. Junquin, E. M. Arenaza-Urquijo, D. Vidal-Pineiro, C. Valls-Pedret, E. M. Palacios, S. Domenech, A. SalvÃ, N. BargallÃş, and D. BartrÃľs-Faz, "Changes in whole-brain functional networks and memory performance in aging," *Neurobiology of Aging*, vol. 35, pp. 2193–2202, Oct. 2014.
22. M. S. Gazzaniga, ed., *The New Cognitive Neurosciences: Second Edition*. The MIT Press, 2 ed., Nov. 1999.
23. D. S. Bassett and M. S. Gazzaniga, "Understanding complexity in the human brain," *Trends in cognitive sciences*, vol. 15, pp. 200–209, May 2011. PMID: 21497128.
24. J. Fuster, "The module: crisis of a paradigm book review, "the new cognitive neurosciences" 2nd edition, m.s. gazzaniga, editor-in-chief, mit press," *Neuron*, no. 26, pp. 51–53, 2000.
25. D. Watts and S. Strogatz, "Collective dynamics of 'small-world' networks," *Nature*, vol. 393, pp. 244–442, 1998.
26. D. S. Bassett and E. Bullmore, "Small-world brain networks," *The Neuroscientist*, vol. 12, pp. 512–523, Dec. 2006.
27. A. Anderson and M. S. Cohen, "Decreased small-world functional network connectivity and clustering across resting state networks in schizophrenia: an fMRI classification tutorial," *Frontiers in Human Neuroscience*, vol. 7, p. 520, 2013.
28. C. J. Stam, "Modern network science of neurological disorders," *Nature Reviews Neuroscience*, vol. 15, pp. 683–695, Oct. 2014.
29. K. Supekar, V. Menon, D. Rubin, M. Musen, and M. D. Greicius, "Network analysis of intrinsic functional brain connectivity in alzheimer's disease," *PLoS Computational Biology*, vol. 4, June 2008. PMID: 18584043 PMCID: PMC2435273.
30. Y. Liu, M. Liang, Y. Zhou, Y. He, Y. Hao, M. Song, C. Yu, H. Liu, Z. Liu, and T. Jiang, "Disrupted small-world networks in schizophrenia," *Brain: a journal of neurology*, vol. 131, pp. 945–961, Apr. 2008. PMID: 18299296.
31. W. Liao, Z. Zhang, Z. Pan, D. Mantini, J. Ding, X. Duan, C. Luo, G. Lu, and H. Chen, "Altered functional connectivity and small-world in mesial temporal lobe epilepsy," *PLoS ONE*, vol. 5, p. e8525, Jan. 2010.
32. Z. Zhang, W. Liao, H. Chen, D. Mantini, J.-R. Ding, Q. Xu, Z. Wang, C. Yuan, G. Chen, Q. Jiao, and G. Lu, "Altered functionalâĂŞstructural coupling of large-scale brain networks in idiopathic generalized epilepsy," *Brain*, vol. 134, pp. 2912–2928, Oct. 2011.
33. J. Goni, M. P. v. d. Heuvel, A. Avena-Koenigsberger, N. V. d. Mendizabal, R. F. Betzel, A. Griffa, P. Hagmann, B. Corominas-Murtra, J.-P. Thiran, and O. Sporns, "Resting-brain functional connectivity predicted by analytic measures of network communication," *Proceedings of the National Academy of Sciences*, vol. 111, pp. 833–838, Jan. 2014.
34. A. Irimia and J. D. Van Horn, "Systematic network lesioning reveals the core white matter scaffold of the human brain," *Frontiers in Human Neuroscience*, vol. 8, p. 51, 2014.
35. V. Latora and M. Marchiori, "Efficient behavior of small-world networks," *Physical Review Letters*, vol. 87, p. 198701, Oct. 2001.
36. Q. Jiao, G. Lu, Z. Zhang, Y. Zhong, Z. Wang, Y. Guo, K. Li, M. Ding, and Y. Liu, "Granger causal influence predicts BOLD activity levels in the default mode network," *Human Brain Mapping*, vol. 32, pp. 154–161, Jan. 2011.
37. N. Tzourio-Mazoyer, B. Landeau, D. Papathanassiou, F. Crivello, O. Etard, N. Delcroix, B. Mazoyer, and M. Joliot, "Automated anatomical labeling of activations in SPM using a macroscopic anatomical parcellation of the MNI MRI single-subject brain," *NeuroImage*, vol. 15, pp. 273–289, Jan. 2002.
38. J. S. Damoiseaux, C. F. Beckmann, E. J. S. Arigita, F. Barkhof, P. Scheltens, C. J. Stam, S. M. Smith, and S. a. R. B. Rombouts, "Reduced resting-state brain activity in the "default network" in normal aging," *Cerebral Cortex (New York, N.Y.: 1991)*, vol. 18, pp. 1856–1864, Aug. 2008.

39. W. Koch, S. Teipel, S. Mueller, K. Buerger, A. L. W. Bokde, H. Hampel, U. Coates, M. Reiser, and T. Meindl, "Effects of aging on default mode network activity in resting state fMRI: does the method of analysis matter?," *NeuroImage*, vol. 51, pp. 280–287, May 2010.
40. S. Vergun, A. S. Deshpande, T. B. Meier, J. Song, D. L. Tudorascu, V. A. Nair, V. Singh, B. B. Biswal, M. E. Meyerand, R. M. Birn, and V. Prabhakaran, "Characterizing Functional Connectivity Differences in Aging Adults using Machine Learning on Resting State fMRI Data," *Frontiers in Computational Neuroscience*, vol. 7, p. 38, 2013.
41. A. Salami, S. Pudas, and L. Nyberg, "Elevated hippocampal resting-state connectivity underlies deficient neurocognitive function in aging," *Proceedings of the National Academy of Sciences*, vol. 111, pp. 17654–17659, Dec. 2014.
42. A. M. Fjell, M. H. Sneve, A. B. Storsve, H. Grydeland, A. Yendiki, and K. B. Walhovd, "Brain Events Underlying Episodic Memory Changes in Aging: A Longitudinal Investigation of Structural and Functional Connectivity," *Cerebral Cortex*, p. bhv102, May 2015.
43. N. A. Crossley, A. Mechelli, J. Scott, F. Carletti, P. T. Fox, P. McGuire, and E. T. Bullmore, "The hubs of the human connectome are generally implicated in the anatomy of brain disorders," *Brain*, vol. 137, pp. 2382–2395, Aug. 2014.